2021

The Thermodynamic Behavior Of Low-GWP Zeotropic Mixtures On Water-Source Heat Pump Equipment

Saad Saleem
Oklahoma State University, saad.saleem@okstate.edu

Craig R. Bradshaw

The thermodynamic behaviour of low-GWP zeotropic mixtures on water-source heat pump equipment

Saad SALEEM[(1)] *, Craig R. BRADSHAW[(2)]

[(1)] [(2)] Oklahoma State University, Mechanical & Aerospace Engineering,
Stillwater, OK 74075, USA
[(1)] saad.saleem@okstate.edu, [(2)] craig.bradshaw@okstate.edu

* Corresponding Author

ABSTRACT

Regulatory changes, aimed at mitigating climate change, are forcing air-conditioning and heat pump manufacturers to change refrigerants in their products, including all Water-Source Heat Pumps (WSHPs). These changes require substantive changes to WSHP equipment design in order to continue to deliver heat pumps that meet product specifications and energy efficiency regulations. Some of the proposed low-GWP refrigerants to replace R410A, such as R452B and R454A, are zeotropic mixtures of refrigerants. Zeotropes with a significant glide may be taken advantage of in the refrigerant-to-water heat exchanger in a WSHP to improve overall system efficiency. However, there is a potential to also reduce system efficiency if not designed appropriately. This work presents a four-component heat pump model which includes a moving boundary condenser model, lumped element evaporator model, and fixed efficiency compressor model. This model was validated against the data of a R410A water-to-water heat pump operated in heating mode with an average 9.7% MAE in prediction of COP. This model was exercised using R452B and R454A and discovered that the latter provided an opportunity to increase the system COP as a result of the increased enthalpy of vaporization of the fluid. Additionally, the moderate glide that these two refrigerants produce is not significant enough to warrant significant consideration for a water-to-water heat pump.

1. INTRODUCTION

Recently, regulations aimed at mitigating climate change, such as the Kigali amendment to the Montreal Protocol, are forcing air conditioning (AC) and Water Source Heat Pumps (WSHPs) to replace the existing halogenated refrigerants (chlorofluorocarbons and hydrofluorocarbons) with more climate friendly alternatives. Some of these alternative low Global Warming Potential (GWP) refrigerants are zeotropic mixtures of refrigerants. Zeotropic mixtures (or non-azeotropic mixtures) are blends of two or more individual components, having different compositions of each component in the vapor and liquid phase at thermodynamic equilibrium as a saturated liquid-vapor mixture. At any given concentration, the zeotropic mixture will condense and boil over a temperature range, termed as a temperature glide. This glide, if matched with the temperature change of the source-side heat transfer fluid in the counter flow heat exchanger of a water source heat pump (WSHP), can result in reducing the thermodynamic irreversibilities in the heat exchangers (condenser and evaporator), as a result of improved heat exchanger effectiveness. The improved heat exchanger effectiveness ultimately transforms into an improved Coefficient of Performance (COP) of the system.

Several theoretical and experimental studies have looked into quantifying the benefits of using low-GWP alternative zeotropic refrigerant mixtures in AC and WSHP equipment originally designed for R410A. Sethi & Motta (2016) evaluated R452B and R447B as drop-in replacements by running simulations on an air-source heat pump, finding that above 35°C, both refrigerants lead to an increase in system efficiency of 3-4%, in comparsion to R410A. (Atilla Gencer Devecioğlu, 2017) evaluated four alternatives for R410A in an air-source heat pump. R452B was observed to be the better alternative to R410A in heating mode, while R466A was more suitable in cooling mode. Chen *et al.*, (2018) investigated the drop-in performance of R452B and R447B in air-to-water heat pumps with a sub-cooler vapor injection cycle designed for R410A. It was found that the improvement in COP of the system for the R452B system is 4-9% and 1.4-2.4%, and that of the R447B system is 3-12% and 0.4-3.8% with and without vapor injection, respectively. Shen *et al.*, (2018) did an experimental and numerical investigation on a rooftop air conditioner (RTU) , to evaluate several drop-in alternatives for R22 and R410A. For R410A, R452B turned out to be a better alternative than R32. This is because with R452B, the required compressor displacement volume and the most optimum heat exchanger geometry configuration was identical to that of R410A, so as to achieve the same system performance. Most recently Devecioğlu & Oruç, (2020) investigated R466A as drop-in alternative to R410A in a variable

refrigerant flow based air-source heat pump and found that it had a COP higher than R410A by 5-15% and 4% in cooling and heating mode, respectively.

The previous studies almost exclusively featured air-source equipment with limited studies of drop-in performance of low-GWP refrigerants in WSHPs. Additionally, of the previous studies that featured WSHPs, none of the the studies included coaxial heat exchangers as the refrigerant-to-water heat exchanger. The present work aims to qauntify the the performance of new low-GWP zeotropic refrigerant mixtures as drop-in replacements for R410A in a WSHP operating in heating mode. A thermodynamic model of a commercial WSHP with a coaxial heat exchanger is developed and initially validated using R410A performance data available from the manufacturer. The model is then exercised by simulating the use of "drop-in" refrigerant alternatives, R454B and R452B, and the results are compared to those obtained with R410A.

2. HEAT PUMP SIMULATION MODEL DEVELOPMENT

Table 1 lists down some high level information on the refrigerants used in this analysis. R454B and R452B were chosen as the "drop-in" alternatives to R410A, because of their lower GWP and thermodynamic properties that are similar to those of R410A.

Table 1: Important characteristics of refrigerants chosen for the analysis

	R410A (base)	**R454B**	**R452B**
Type	HFC	HFO	HFO/HFC blend
Global Warming Potential (GWP)	2088	467	676
Ozone Depleting Potential (ODP)	0	0	0
ASHRAE safety class	A1	A2L	A2L
Glide* (K)	0.1	1.4	1.2

** The temperature glide is based on a simple thermodynamic cycle operating between an average evaporating temperature of 11.7°C with 8.3 K of superheat and an average condensing temperature of 46.1 C with 8.3 K of subcooling; the isentropic efficiency of the compressor is assumed to be 0.7*

The thermodynamic heat pump model was based on the basic vapor compression cycle, and it includes a moving boundary condenser model, lumped evaporator model and a fixed efficiency compressor model. Both heat exchangers are solved on the basis of the Effectiveness-NTU method. The condenser had more fidelity than the evaporator, so as to better capture the influence of temperature glide in heating mode. The model was developed in Engineering Equation Solver (EES) (Klein, 2019) due to its user friendliness and a wide range of properties for several fluids. The fundamental assumptions for each of the model components are listed in Table 2.

Table 2: Major assumptions for all the components in the thermodynamic heat pump model

Component	**Assumption**
Compressor	Fixed isentropic and volumetric efficiency
Evaporator	No pressure drop on water or refrigerant side
	No circulation of oil with refrigerant
Condenser	No pressure drop on water or refrigerant side
	No circulation of oil with refrigerant
Expansion device	No heat gains during expansion process

Additionally, it is assumed that: (1) pressure of water on the load and source side of system is equal to atmospheric pressure, (2) thermodynamic and transport properties of water along the heat exchangers are assumed constant, and (3) tube conduction is negligible.

All component models were initially written independently. Figures 1, 2 and, 3 show the inputs, outputs and parameters for the condenser, evaporater and compressor models respectively. Note that the expansion valve was modelled as an isenthalpic expansion process from condenser discharge to the evaporater suction.

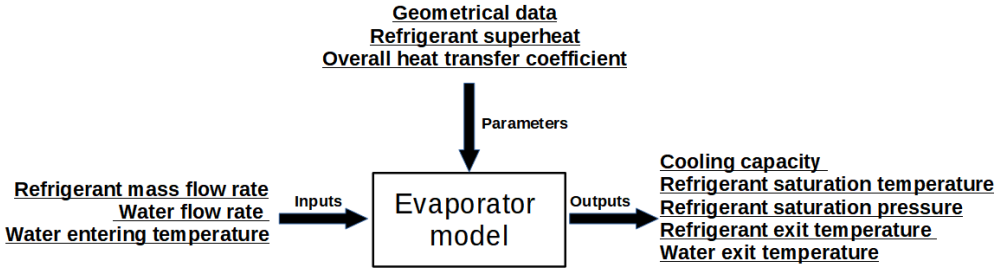

Figure 1. Inputs, outputs and parameters for the lumped evaporator model

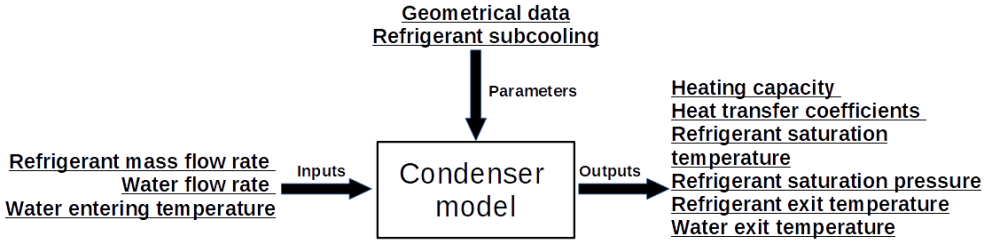

Figure 2. Inputs, outputs and parameters for the moving boundary condenser model

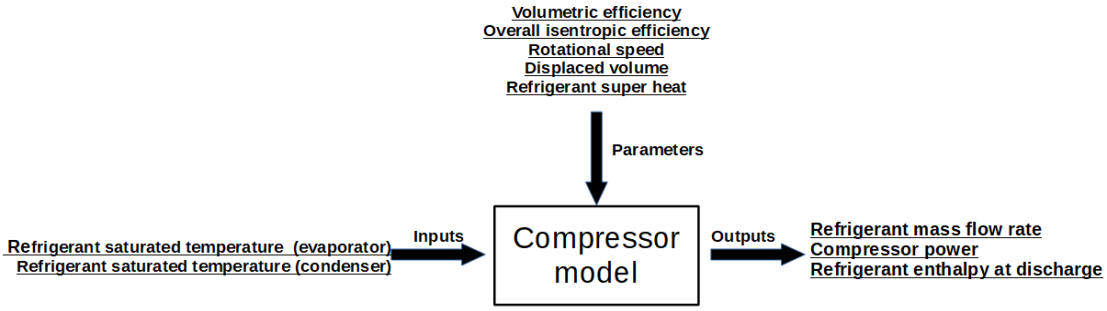

Figure 3. Inputs, outputs and parameters for the fixed efficiency compressor model

Finally, all individual models were combined together. Figure 4 shows how the various components communicate with each other in order to solve the entire heat pump model.

3. BASE MODEL TUNING AND VALIDATION

To ensure that any predictions made by the heat pump model were reasonably accurate, the model was validated by comparing its predictions against a published datasheet of for a commercially available, R410A, water-to-water heat pump with two identical coaxial heat exchangers and a single, fixed speed, scroll compressor. The specifications of the heat pump are shown in Table 3.

Table 3: Specifications and Performance Data of the WSHP used for model validation

Cooling mode (Indoor 12°C (53.6°F) and outdoor 30°C (86°F))	**Capacity**	9.47 kW (32,300 Btu/hour)
	EER	4.28 W/W (14.6 Btu/hour/W)
Heating mode (Indoor 40°C (104°F) and outdoor 20°C (68°F))	**Capacity**	12.64 kW (32,300 Btu/hour)
	COP	4.90

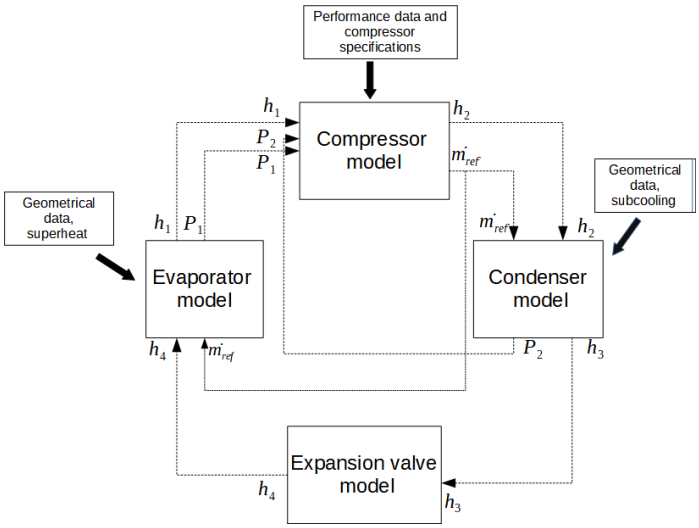

Figure 4: Flow of information in the heat pump simulation model

Table 4 shows the range of the input variables (otained from the performance datashet) the model was simulated for using R410A as the refrigerant. A superheating and subcooling of 10°C were provided as inputs to the model and were kept constant in all simulations.

Table 4: Range of input variables the initial model was simulated for

Source (evaporator) side inputs		**Load (condenser) side inputs**	
Entering Water Temperature (°C)	**Water flow rate (kg/s)**	**Entering Water Temperature (°C)**	**Water flow rate (kg/s)**
-6.67	0.567	15.6, 26.7, 37.8	0.284, 0.428, 0.567
4.44	0.284	15.6, 26.7, 37.8	0.284, 0.428, 0.567
	0.428	15.6, 26.7, 37.8	0.284, 0.428, 0.567
	0.567	15.6, 26.7, 37.8	0.284, 0.428, 0.567
15.6	0.284	15.6, 26.7, 37.8	0.284, 0.428, 0.567
	0.428	15.6, 26.7, 37.8	0.284, 0.428, 0.567
	0.567	15.6, 26.7, 37.8	0.284, 0.428, 0.567
26.7	0.284	15.6, 26.7, 37.8	0.284, 0.428, 0.567
	0.428	15.6, 26.7, 37.8	0.284, 0.428, 0.567
	0.567	15.6, 26.7, 37.8	0.284, 0.428, 0.567

No information was provided by the WSHP manufacturer about the surface areas of the (identical) heat exchanger. In order to estimate this value to provide as an input to the heat pump model, it was assumed that the coil length of the heat exchanger is directly proportional to the surface areas, calculated by using Equation (1).

$$A_{cond} = A_{evap} = A_{density} * L \quad (1)$$

The coil length of the heat exchanger is calculated using Equation (2).

$$L = \pi * N_{coax} * D_{coax} \quad (2)$$

The heat exchanger had an outer diameter of 0.35 m and a total of 2 rounds, and hence the circumference (length) came out to be 2.1 m.

The simulation model was tuned for reasonably predicting the actual heat pump performance (from the performance data) by iterating on the heat exchanger surface areas and on a correction factor (multiplied by the heat transfers in evaporator and condenser) until the Mean Absolute Percentage Error (MAPE) for the heating (condenser) capacity and compressor power were no more than 3% and 10% respectively. After undergoing the process explained above, the optimum value of the heat exchanger areas came out to be $3m^2$, while the value for the correction factors (applied to heat transfers in condenser and evaporator) came out to be 0.7.

Table 5 presents the complete results of the base model comparison listed as the percentage of the maximum, minimum and absolute errors obtained between the model predictions and datasheet values of condenser capacity and compressor power input, by running the model for the range of input variables shown in Table 4.

Table 5: Comparison of simulated and actual (datasheet) values of condenser capacity and compressor input power

Parameter	Load flow rate (kg/s)	MAPE (%)
Condenser capacity	0.284	2.8%
	0.428	2.3%
	0.567	2.3%
Compressor input power	0.284	7.4%
	0.428	8.1%
	0.567	9.1%

The compressor model was independently compared against the compressor datasheet, the MAPE for which came out to be only 3.9%, whereas it was a high as 9.1% (Table 5) when validating the heat pump model against the compressor power in the heat pump`s datasheet. This indicated that part, but not all, of the error in the compressor power predictions in the heat pump model was due to assuming fixed isentropic and volumetric efficiencies.

The simulated and actual heat pump COP were also compared and it was found that the overall MAPE between the results was 7.14%, 8.4% and 9.3% for load flow rates of 0.284 kg/s, 0.428 kg/s and 0.567 kg/s respectively. Thus, an average MAE of 8.3% in COP prediction and the overall MAPE trends between simulated and actual (datasheet) suggest that the model will be reliable for comparing performance for various refrigerants and look for trends in the results.

4. "DROP-IN" SIMULATION RESULTS

After validating the heat pump model, simulations were run for all three refrigerants (R410A, R452B and R454B) chosen for the analysis. The source (evaporator) side inlet water temperature and flow rate were kept constant, while on the load (condenser) side, the entering water temperature (EWT) was varied for three water flow rates, as shown in Table 6. These parameters are within the bounds for which the base model was validated in section 3.

Table 6: Range of inlet variables for comparison of simulations for the different refrigerants

Source EWT (°C)	Source Flow rate (kg/s)	Load EWT (°C)	Load flow rate (kg/s)
4.44	0.567	10.0-32.2	0.284, 0.428, 0.567

Condenser capacity, compressor power and system COP were used as the main performance parameters. Figures 5, 6 and, 7 show how the predicted condenser capacity, compressor work input and system COP varied for the three refrigerants respectively, as a function of load side EWT for three different load flow rates.

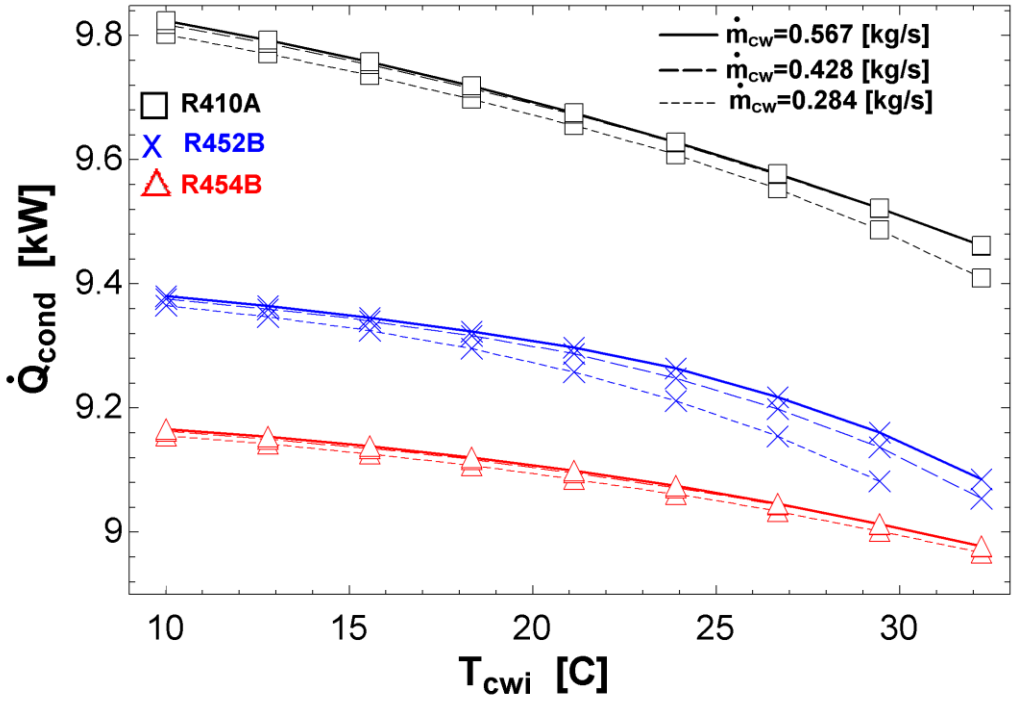

Figure 5: Comparison of simulated condenser capacity for varying entering water temperature and three flow rates

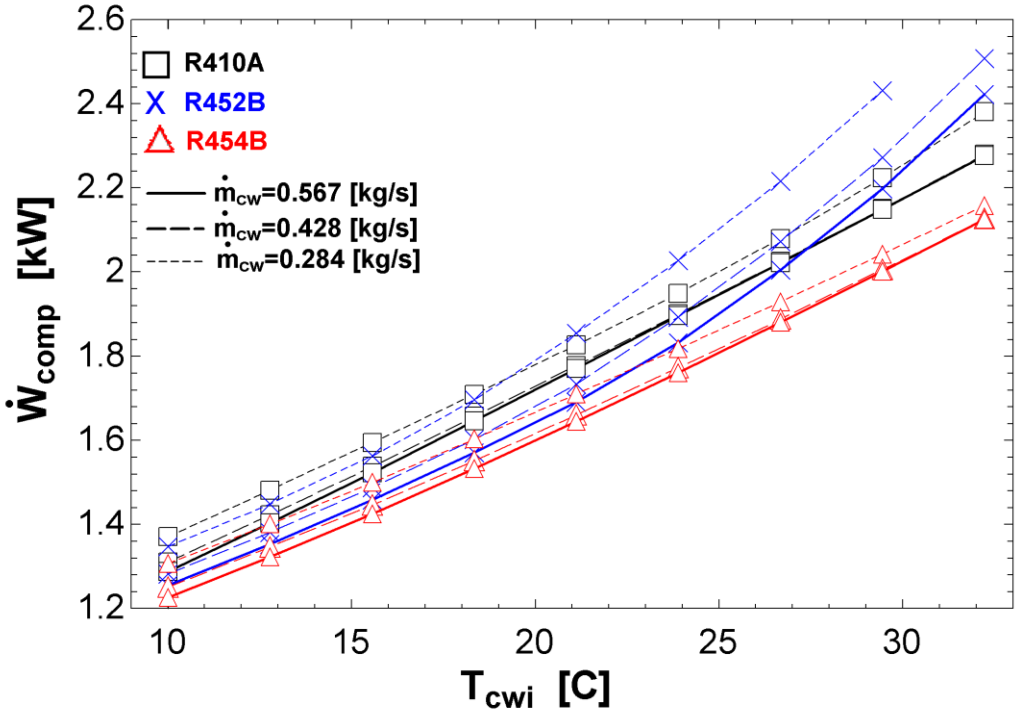

Figure 6: Comparison of simulated compressor power for varying entering water temperature and three flow rates

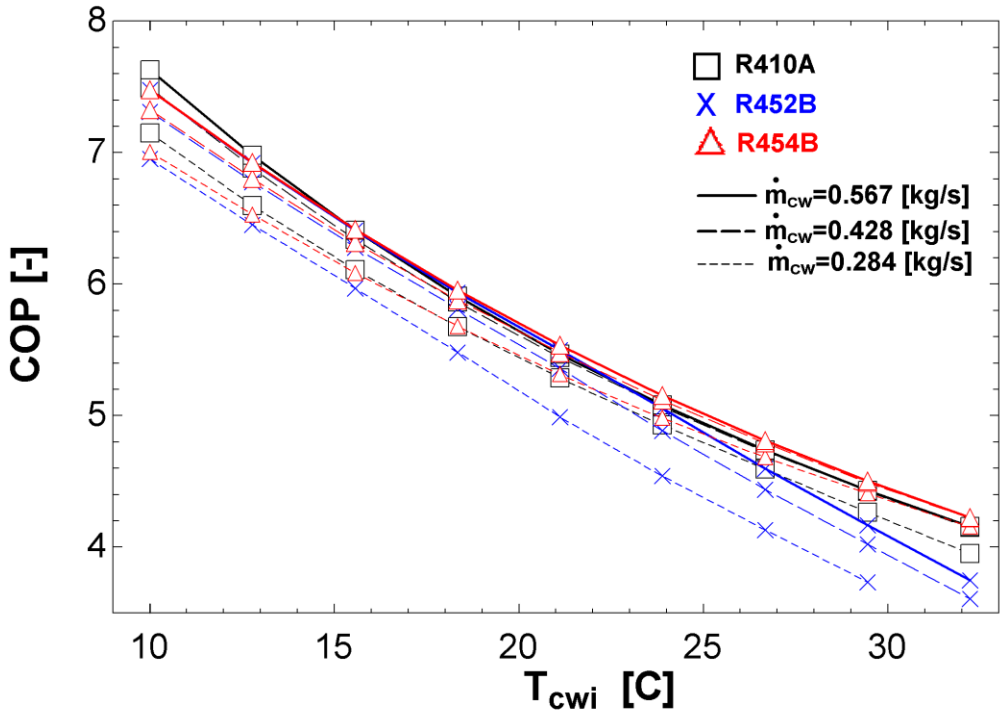

Figure 7: Comparison of simulated system COP for varying entering water temperature and three flow rates

From Figure 5, it can be seen that the heating capacity is highest for R410A, followed by R452B and R454B. Interestingly, R410A has the lowest temperature glide whereas R454B has the highest. Figure 6 shows that in general, R454B requires the smallest compressor work input, at all load flow rates, when compared to R410A and R452B. An odd phenomenon is observed in the trends of R410A and R452B; initially the former has a higher compressor work input than the latter, but beyond EWT of 19°C, the trends reverse. Figure 7 shows that for the lower condenser EWTs, i.e. < 19°C, R410A has the highest COP, followed by R454B and finally by R452B. However, for higher EWTs, R454B has the highest COP and that of R410A drops to 2nd in line.

In order to investigate the reasoning behind the trends in Figures 5 to 7, trends in several other variables were observed as a function of increasing EWT to condenser at the three load flow rates, namely:

(1) Refrigerant flow rate, given by,

$$\dot{m}_{ref} = \eta_{vol} * \rho_{suc} * V_{disp} * \omega \quad (3)$$

(2) Enthalpy change across condenser, which is obtained from the overall condenser capacity, given by,

$$\dot{Q}_{cond} = \dot{m}_{ref} * (h_2 - h_3) \quad (4)$$

(3) Enthalpy change across compressor, given by,

$$h_2 - h_1 = (1 - f_Q) * \dot{W}_{comp}/\eta_{iso} \quad (5)[1]$$

[1] The value of the heat loss factor, f_Q , in equation (5) for the compressor in all analysis is assumed to be 0.2, which is a value generally applicable for small to medium size hermetic compressors.

Figures 8, 9 and, 10 show the afore mentioned variables plotted against EWT for a load flow rate of 0.284 kg/s. Additionally, the pinch point temperature difference (PPTD) between the three refrigerants and water were plotted against entering condenser water temperature , also for a load flow rate of 0.284 kg/s, shown in Figure 11.

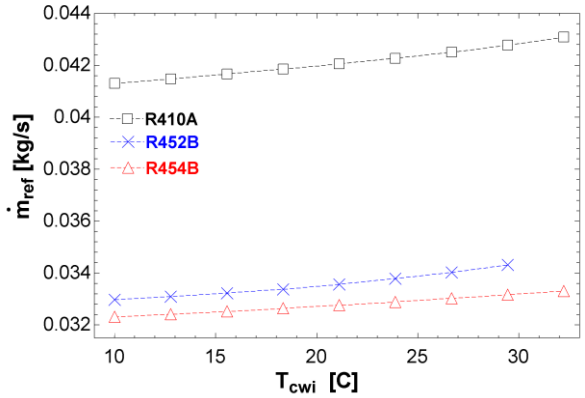

Figure 8: Comparison of simulated refrigerant flow rate for varying entering water temperature and load flow rate of 0.284 kg/s

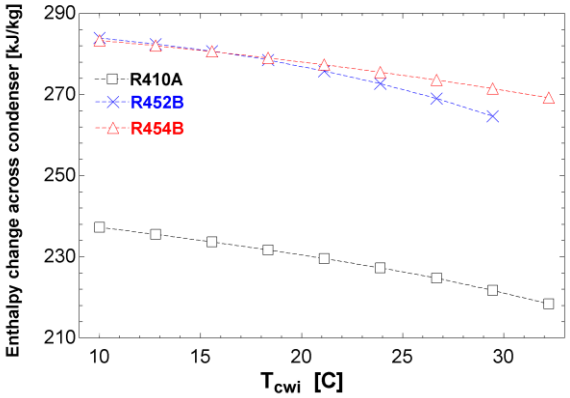

Figure 9: Comparison of simulated enthalpy change across condenser for varying entering water temperature and load flow rate of 0.284 kg/s

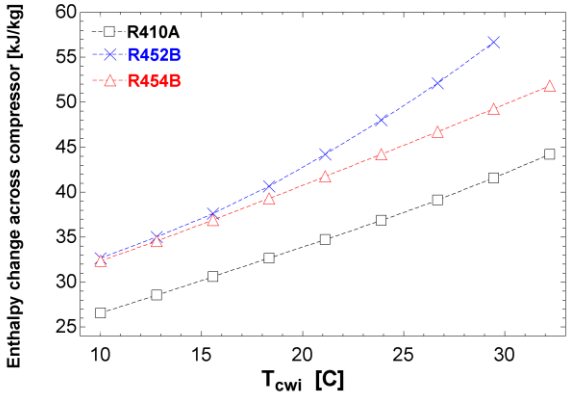

Figure 10: Comparison of simulated enthalpy change across compressor for varying entering water temperature and load flow rate of 0.284 kg/s

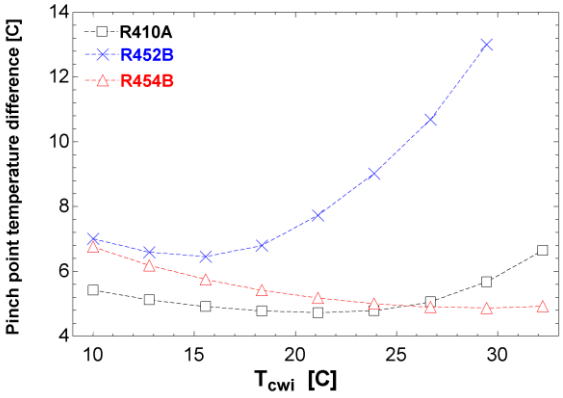

Figure 11: Comparison of simulated pinch point temperature difference across condenser for varying entering water temperature and load flow rate of 0.284kg/s

It was found that across the test entire test matrix (see Table 6), R452B had an average 20% lower refrigerant flow rate than R410A, while R454B had an average 22% lower refrigerant flow rate. On the other hand, enthalpy change in the condenser for R452B and R454B on average is greater by 19% and 21% respectively when compared to R410A. By referring back to Figure 5, it is evident that combined effect of the above two factors caused the condenser capacities for R452B and R454B to be lower by 4% and 6% respectively when compared to that for R410A.

The results additionally show that the enthalpy change across compressor is lowest for R410A. This factor, combined with its relatively higher flow rate, helps to explain why its compressor work input is between that of R452B and R454B. The PPTD shows an overall trend of initial decrease and then increase for all three fluids. In case of R454B, it did not increase within the range of EWTs in the test matrix, thus causing it to have the lowest PPTD, followed by R410A and then R452B, as seen in Figure 11. R454B presents with roughly 1.5°C lower PPTD compared with R410, whereas R452B has as high as 6°C higher PPTD. The fluid with the lowest PPTD has the lowest amount of thermodynamic irreversibilities. Figure 7 confirms this by presenting the overall system COP, which correlates strongly with the inverse of PPTD. For R454B, the results suggest that the existing heat exchanger provides lower

irreversibilities compared with R410A under some conditions, it could therefore have its area reduced without significant reduction in COP as a potential cost savings.

It can be observed that the alternative zeotropic refrigerants simulated in this study did not lead to an improved system performance when simply used as "drop-in" replacements in a system designed for R410A. Thus, design modifications would be necessary to fully leverage these low-GWP zeotropic mixtures. One proposed modification, as per the results in Figure 11, can be to reduce the effective surface area of an R410A heat exchanger when using R454B as the "drop-in" replacement, so as to match the heating capacity originally provided by R410A. To investigate another possible modification, a small parametric study was done for R454B for a single set of inlet conditions. By increasing the compressor displacement by 8.9%, the condenser capacity (shown in Figure 5) increased by 7%, i.e. from 9.2 kW to 9.8 kW, to match that of R410A at the same inlet conditions.

5. CONCLUSIONS

In this paper, a comparative study has been performed to explore the influence of using the zeotropic refrigerant mixtures, R452B and R454B as "drop-in" replacements for a 3 ton WSHP designed for R410A, by means of a numerical thermodynamic model.

Overall, the analysis showed that simply using "drop-in" low-GWP replacements in existing WSHP may produce modest improvements or reductions in efficiency. It was found that, with high load-side water flow rates, the COP increased by as much as 5% with R454B when compared to using R410A. R452B had a lower COP when compared to R410A during all the simulations.

Both the drop-in alternatives result in lower heating capacity compared with R410A in all simulations; R454B has the lowest capacity degradation (6%) despite having the highest COP with R452B having a 4% reduction. The reduction in capacity of both fluids would require an increase in compressor displacement for applications where heating capacity is critical. The heat exchange efficiency of the two fluids also presented with modest differences. The pinch point temperatures of R454B were always higher than that of R410A where there were some operating conditions where R454B showed as much as a 1.5°C reduction in pinch point temperature. This suggests that heat exchange surface should be added to a R452B system where R454B systems may allow a reduction in coil surface area to save cost.

NOMENCLATURE

$\boldsymbol{A}$	Area (m^2)	**Subscripts**	
$\boldsymbol{D}$	Diameter (m)	$\boldsymbol{coax}$	Coaxial heat exchanger
$\boldsymbol{f_Q}$	Heat loss factor (-)	$\boldsymbol{c, cond}$	Condenser
$\boldsymbol{L}$	Coil length (m)	$\boldsymbol{comp}$	Compressor
$\boldsymbol{\dot{m}}$	Mass flow rate (kg/s)	$\boldsymbol{evap}$	Evaporator
$\boldsymbol{N}$	Number (-)	$\boldsymbol{i}$	In
$\boldsymbol{\dot{Q}}$	Capacity (kW)	$\boldsymbol{iso}$	Isentropic
$\boldsymbol{\dot{W}}$	Work (kW)	$\boldsymbol{suc}$	Suction
$\boldsymbol{V_{disp}}$	Volumetric displacement (m^3)	$\boldsymbol{vol}$	Volumetric
		$\boldsymbol{w}$	Water
Greek symbols		**1**	State point 1 - Suction of compressor
$\boldsymbol{\eta}$	Efficiency	**2**	State point 2 - Discharge of compressor
$\boldsymbol{\rho}$	Density (kg/m^3)	**3**	State point 3 - Exit of condenser
$\boldsymbol{\omega}$	Rotational speed (rad/s)	**4**	State point 4 - Inlet of evaporator

Acronyms

AC	Air Conditioning
ASHRAE	American Society of Heating, Refrigeration and Air Conditioning Engineers
COP	Coefficient of Performance
EER	Energy Efficiency Ratio

EES	Engineering Equation Solver
EWT	Entering Water Temperature
GWP	Global Warming Potential
HVAC	Heating, Ventilation and Air Conditioning
HFC	Hydrofluorocarbon
HFO	Hydrofluoroolefin
HCFC	Hydro chlorofluorocarbon
MAE	Mean Absolute Error
NTU	Number of Transfer Units
PPTD	Pinch Point Temperature Difference
WSHP	Water Source Heat Pump

REFERENCES

Chen, X., Yang, J., Liu, C., & Chen, J. (2018). Heating performance comparison of R410A and its substitutions in air-to-water heat pumps with vapor injection. *International Journal of Refrigeration*, *96*, 78–87. https://doi.org/10.1016/j.ijrefrig.2018.09.007

Devecioğlu, Atilla G., & Oruç, V. (2020). Energetic performance analysis of R466A as an alternative to R410A in VRF systems. *Engineering Science and Technology, an International Journal*, *23*(6), 1425–1433. https://doi.org/10.1016/j.jestch.2020.04.003

Devecioğlu, Atilla Gencer. (2017). Seasonal performance assessment of refrigerants with low GWP as substitutes for R410A in heat pump air conditioning devices. *Applied Thermal Engineering*, *125*, 401–411. https://doi.org/10.1016/j.applthermaleng.2017.07.034

Klein, S. A. (2019). Engineering Equation Solver, Academic Professional V10.644-3D. F-Chart Software.

Sethi, A., & Motta, S. F. Y. (2016). Low GWP Refrigerants for Air-conditioning and Chiller Applications. *International Compressor Engineering, Refrigeration and Air Conditioning, and High Performance Buildings Conferences*, *2*(2013), 1–8.

Shen, B., Abdelaziz, O., Shrestha, S., & Elatar, A. (2018). Model-based optimizations of packaged rooftop air conditioners using low global warming potential refrigerants. *International Journal of Refrigeration*, *87*, 106–117. https://doi.org/10.1016/j.ijrefrig.2017.10.028